Renewable and Sustainable Energy Reviews 19 (2013) 444–453

Contents lists available at SciVerse ScienceDirect

Renewable and Sustainable Energy Reviews

journal homepage: www.elsevier.com/locate/rser

An overview for the heat transfer performance of HFO-1234yf

Chi-Chuan Wang *

Department of Mechanical Engineering, National Chiao Tung University, Hsinchu 300, Taiwan

ARTICLE INFO

Article history:
Received 1 May 2012
Received in revised form
15 November 2012
Accepted 19 November 2012
Available online 12 December 2012

Keywords:
HFO-1234yf
R-134a
Two-phase heat transfer coefficient
Pressure drop
Flow pattern

ABSTRACT

This study provides an overview about the two-phase heat transfer performance for HFO-1234yf which is made to substitute R-134a. Based on the limited information, it is found that the nucleate boiling heat transfer coefficient (HTC) and convective boiling HTC for HFO-1234yf are comparable to R-134a provided $q < 200\ \mathrm{kW\ m^{-2}}$. The critical heat flux for HFO-1234yf is about 20–40% lower than that of R-134a. For external condensation, the only database shows that the HTC between HFO-1234yf and R-134a is also negligible. However, it is found that the major thermophysical properties influencing condensing HTC suggest a lower HTC of HFO-1234yf. For in-tube condensation, it is found that the condensation HTCs for HFO-1234yf are inferior to those of R-134a, and the difference increases with the rise of vapor quality. The predictive correlations applicable for pressured drop for HFO-1234yf are not consistent, it is probably attributed to the difference in tube diameter in the publications.

Contents

1. Introduction

HydroFluoroCarbon (HFC) refrigerants had substituted ChloroFluoroCarbon (CFC) and HydroChloroFluoroCarbon (HCFC) refrigerants due to environmental concerns of harming the Ozone Depletion Potential (ODP) since 1990. However, HFC refrigerants such as R-134a, R-410A, R-407C and R-404A have high global warming potential (GWP) over 1000. Hence there is a need to replace HFC refrigerants with high GWP. Yet the European Union has already fixed the limit for mobile air conditioning systems to a GWP of 150.

Vehicle air conditioning is a significant and growing source of greenhouse gas (GHG) pollution. At present stage, most mobile air conditioning (MAC) systems use R-134a as the working fluid whose 100-yr global warming potential (GWP) is as high as 1,430 and MAC is the largest and most emissive sales market for R-134a [1]. As a result, efforts were made to search for new refrigerants that is environmentally benign and can be used to globally replace refrigerants used in future mobile (cars and light trucks) air conditioning systems. Among the candidates, HFO-1234yf is regarded as the promising candidate for its GWP is as low as 4. The thermophysical properties, cycle performance, and two-phase heat transfer performance of HFO-1234yf are the key parameters to estimate the feasibility of using this new refrigerant in mobile air conditioners. The thermophysical properties of refrigerant mixture were reported to be similar to those of R-134a [2], thereby offering an opportunity as a drop-in solution

* Tel.: +886 3 5917 121 x55105; fax: +886 3 5720 634.
E-mail address: ccwang@mail.nctu.edu.tw

1364-0321/$ - see front matter © 2012 Elsevier Ltd. All rights reserved.
http://dx.doi.org/10.1016/j.rser.2012.11.049

Nomenclature

A	surface area (m^2)
CHF	critical heat flux ($W\,m^{-2}$)
C_p	specific heat ($J\,kg^{-1}\,K^{-1}$)
D, d	diameter (m)
G	mass velocity ($kg\,m^{-2}\,s^{-1}$)
g	gravitational acceleration ($m^2\,s^{-1}$)
H	heat transfer coefficient ($W\,m^{-2}\,K^{-1}$)
i	specific enthalpy ($kJ\,kg^{-1}$)
k	thermal conductivity ($W\,m^{-1}\,K^{-1}$)
f	friction factor
Re	Reynolds number, dimensionless
P	pressure (Pa)
P_s	saturation pressure (Pa)
Pr	Prandtl number, dimensionless
P^*	reduced pressure
Q	heat transfer rate (W)
q	heat flux ($W\,m^{-2}$)
T	temperature (°C)
T_s	saturation temperature (°C)
x	vapor quality, dimensionless
X	Lockhart Martinelli parameter, dimensionless
z	axial direction (m)
Z	$=\left(\frac{1-x}{x}\right)^{0.8}(P^*)^{0.4}$

Greek letters

μ	viscosity ($kg\,m^{-1}\,s^{-1}$)
ϕ	two-phase multiplier, dimensionless
σ	surface tension ($N\,m^{-1}$)
ρ	density ($kg\,m^{-3}$)

Subscripts

c	condensation
G	vapor phase
LG	difference between liquid phase and vapor phase
i	inside
L	liquid phase
o	outside
s	saturated
w	wall

for current mobile air conditioners. Fig. 1 shows the relationships between saturation pressure and saturation temperature for various refrigerants (CO_2, R-410A, R-407C, R-22, R-134a, and HFO-1234yf). It appears that R-134a nearly coincides with HFO-1234yf). Normally a drop-in solution yields a lower system performance for lacking optimization. For instance, Lee and Jung [3] had shown that the coefficient of performance and capacity of HFO-1234yf are up to 2.7% and 4.0% lower than those of R-134a, respectively, during a typical drop-in experiment. The compressor discharge temperature and amount of charge of HFO-1234yf are 6.5 °C and 10% lower than those of R-134a. Analogous results were also reported by Zilio et al. [4] and Jarall [5] who also showed a slight decrease in COP for HFO-1234yf system at a same cooling capacity with R-134a.

For further optimizing the system performance, it would need further details in designing the heat exchangers (condenser and evaporator). As a consequence, information about the two-phase heat transfer performance in the heat exchangers (condensation, evaporation, boiling, flow pattern, and pressure drop) plays a detrimental role in optimizing the heat exchangers. Hence, it is important to know whether the actual two-phase characteristics for HFO-1234yf are comparable with that of R-134a. In this regard, it is the objective of this study to provide an overview concerning the two-phase heat transfer performance for HFO-1234yf based on published literatures.

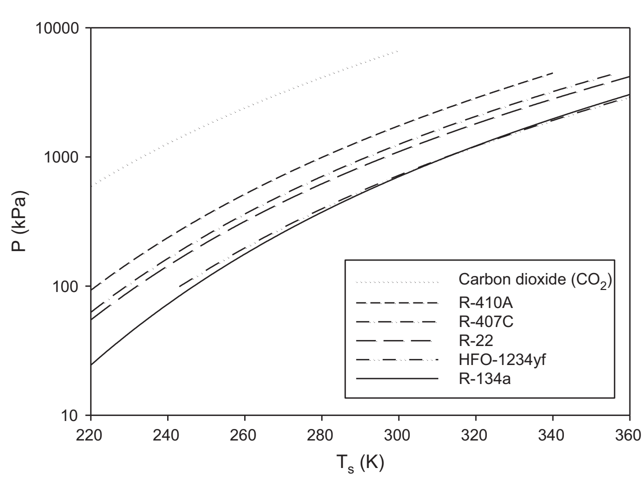


Fig. 1. Relationship between saturation pressure and saturation temperature for various refrigerants.

2. Heat transfer performance for HFO-1234yf

Until now, only very limited information associated with the two-phase heat transfer characteristics as far as HFO-1234yf are concerned. The only published literatures regarding to the two-phase flow characteristics are from Moreno et al. [6] and Park and Jung [7] concerning nucleate boiling, Park et al. [8] for external condensation, Saitoh et al. [9], Li et al. [10] and Mortada et al. [11] regarding to in-tube evaporation, Padilla et al. [12,13] in association with two-phase flow pattern, and Col et al. [14] and Wang et al. [15] for in-tube condensation. The following is a brief summary and discussion from the aforementioned results associated with R-134a counterpart.

2.1. Results for nucleate boiling

Moreno et al. [6] conducted pool boiling experiments for HFO-1234yf and R-134a at system pressures ranging from 0.7 to 1.7 MPa using horizontally oriented 1 cm^2 heat sources. The test surfaces include a plain and microporous surfaces. Test results for T_s=40 and 60 °C are depicted in Fig. 2. And it shows that the boiling heat transfer coefficients of HFO-1234yf and R-134a are nearly identical at lower heat fluxes ($q<200\,kW\,m^{-2}$) while HFO-1234yf yielded lower heat transfer coefficients at higher heat fluxes and lower critical heat flux (CHF) as compared with R-134a.

It is often recognized that three mechanisms, namely bubble agitation, vapor-liquid change phenomenon, and evaporation are associated with basic mechanisms of the nucleate boiling heat transfer [16]. As shown in Table 1a [2,17], the HFO-1234yf has a higher reduced pressure at the same saturation temperature. This is because its critical pressure is about 17% lower than of R-134a. In fact, at a saturation temperature of 40 °C the reduced pressure p^* is approximately 20% higher than that of R-134a, thereby

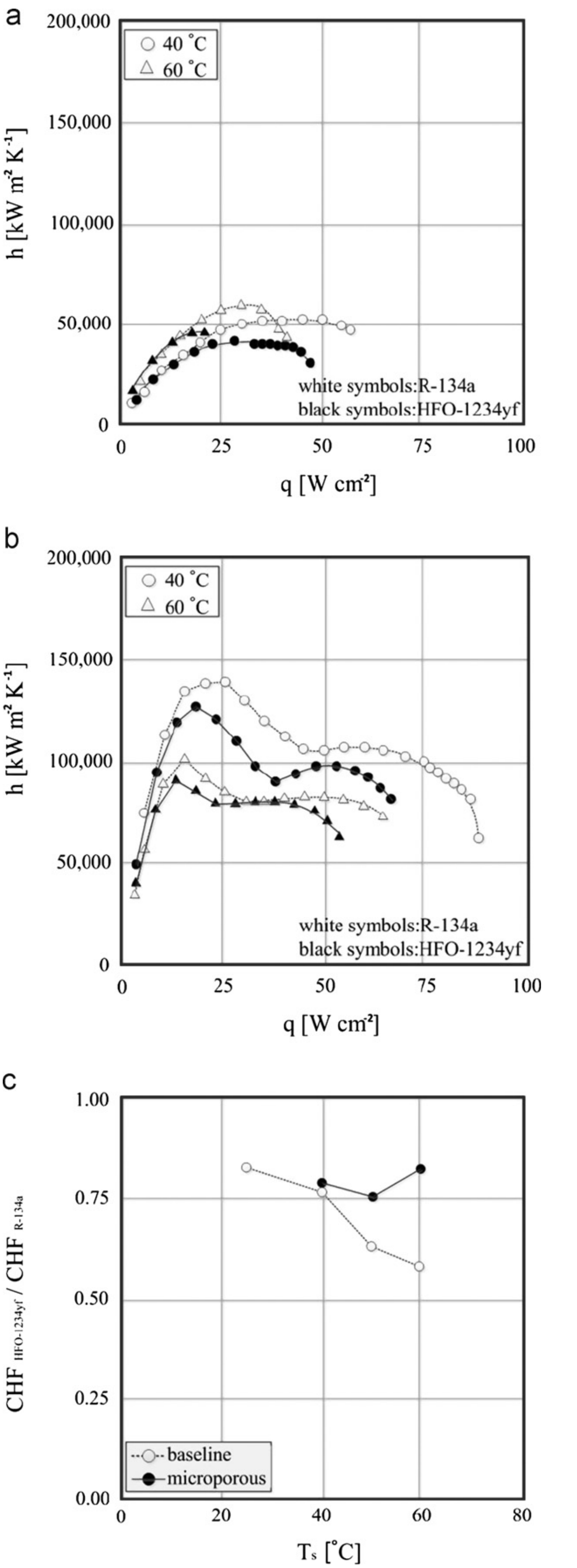


Fig. 2. Nucleate boiling HTCs of HFC-134a and HFO-1234yf for smooth and microporous surfaces (from Moreno et al. [6]). (a) Nucleate boiling HTC vs. *q* for smooth surface. (b) Nucleate boiling HTC vs. *q* for microporous surface. (c) Ratio of critical heat flux for smooth and microporous surface.

Table 1a
Fundamental constants of HFO-1234yf.

	Molecular weight ($g\ mol^{-1)}$	Critical temperature (K)	Critical pressure (Mpa)
R-134a	102	374.13	4.07
R-1234yf	114.042	367.85	3.382

leading to a larger activation sites that would boost the heat transfer coefficient.

On the other hand, the smaller bubble departure diameter $\left(\sim\left(\frac{\sigma}{g(\rho_L-\rho_G)}\right)^{0.5}\right)$ of HFO-1234yf implies a lower bubble agitation, and a smaller vapor–liquid change contribution which offset the positive contribution from the higher reduced pressure. As a result, an almost identical heat transfer coefficient amid R-134a and HFO-1234yf is seen when $q<200\ kW\ m^{-2}$. On the other hand, it appears that the heat transfer coefficient for R-134a gradually surpass those of HFO-1234yf when q is above $200\ kW\ m^{-2}$. Moreno et al. [6] reported that the CHF for HFO-1234yf is appreciably lower than that of R-134a as shown in Fig. 2(c). Therefore they argued that at a higher heat flux (e.g., $q>200\ kW\ m^{-2}$) it is likely that the departure of HTC between R-134a and HFO-1234yf is mainly due to the local dryout of HFO-1234yf.

Analogous results are also applicable in microporous surface (Fig. 2(b)). However, the effect of saturation temperature on HTC for the baseline surface (smooth) and microporous surface is opposite. For the baseline surface (smooth surface), higher saturation temperature brings about higher heat transfer coefficient due to larger activation sites. On the other hand, the activation sites for microporous surface are mainly controlled by the artificial cavity, thereby lifting the positive contribution of cavity activation, and a reversed influence of saturation temperature.

Park and Jung [7] also reported nucleate boiling heat transfer coefficients (HTCs) of R-134a and HFO-1234yf on a flat plain and low fin surfaces. All data were taken at the liquid pool temperature of 7 °C on a small horizontal square copper plate (9.53×9.53 mm) at heat fluxes from 10 to 200 $kW\ m^{-2}$ with an interval of 10 $kW\ m^{-2}$. Test results show that the nucleate boiling HTCs of HFO-1234yf are very similar to those of R-134a for two surfaces tested as depicted in Fig. 3(a). And Park and Jung [7] also found that the conventional boiling correlations can be used for the design of evaporators and boilers with HFO-1234yf. Notice that the maximum test range for their experiments fall within the "identical range" where no appreciable distinction is observed as reported from Moreno et al. [6]. The present study had compared the nucleate boiling HTC for R-134a and HFO-1234yf using the well-known Cooper correlation [18] as shown in Fig. 3(b). The results suggest that the nucleate boiling HTC of HFO-1234yf is marginally higher than that of R-134a.

2.2. *Results of outside condensation*

Park et al. [8] conducted experiments concerning external condensation experiments for plain, low fin, and Turbo-C tubes at a saturated vapor temperature of 39 °C with the wall subcooling ranging from 3 to 8 °C. The geometry of the test tubes is shown in Table 2. Test results show that the condensation HTCs of HFO-1234yf are very similar to those of R-134a for all three surfaces tested as shown in Fig. 4(a). At first glance, it seems that the condensation HTCs for HFO-1234yf is also identical to that of R-134 as those shown in nucleate boiling. However, the authors

Table 1b
Thermodynamic and transport properties of HFC-1234yf.

T (°C)	Fluid	P (kPa)	ρ_L (kg m^{-3})	ρ_G (kg m^{-3})	μ_L (μPa s^{-1})	μ_G (μPa s^{-1})	k_L (W m^{-1} K^{-1})	k_G (W m^{-1} K^{-1})	i_{LG} (kJ kg^{-1})	σ (N m^{-1})	Cp_L (kJ kg^{-1} K^{-1})	Cp_G (kJ kg^{-1} K^{-1})
0	R-134a	292.8	1295	14.43	271.1	10.73	0.092	0.01151	198.6	0.01156	1.341	0.0897
	R-1234yf	315	1175	17.17	220	11.44	0.0746	0.0091	162.3	0.0093	1.259	0.933
5	R-134a	350	1278	17.14	254.4	10.94	0.0898	0.01195	194.8	0.01085	1.355	0.921
	R-1234yf	372	1160	20.8	206	11.67	0.073	0.0094	159	0.00868	1.275	0.957
10	R-134a	414.6	1261	20.23	238.8	11.15	0.0876	0.0124	190.7	0.01014	1.37	0.946
	R-1234yf	436	1144	24.4	194	11.9	0.0713	0.0098	155.6	0.0081	1.293	0.983
20	R-134a	571.7	1225	27.78	210.7	11.58	0.0833	0.01333	182.2	0.00876	1.405	1.001
	R-1234yf	590	1111	33	171	12.36	0.0672	0.0106	148.3	0.0067	1.332	1.041
30	R-134a	770.2	1187	37.54	185.8	12.04	0.079	0.01433	173.1	0.00742	1.446	1.065
	R-1234yf	782	1075	44	152	12.86	0.0631	0.01143	140.1	0.00563	1.379	1.11
40	R-134a	1017	1147	50.09	163.4	12.55	0.0747	0.01544	163	0.0061	1.498	1.145
	R-1234yf	1017	1037	58.3	134	13.49	0.0586	0.0123	131.1	0.00462	1.437	1.196
50	R-134a	1318	1102	66.27	143.1	13.12	0.0704	0.01672	151.8	0.0048	1.566	1.246
	R-1234yf	1301	993.3	76.7	118	14.12	0.054	0.01326	120.9	0.0035	1.515	1.31

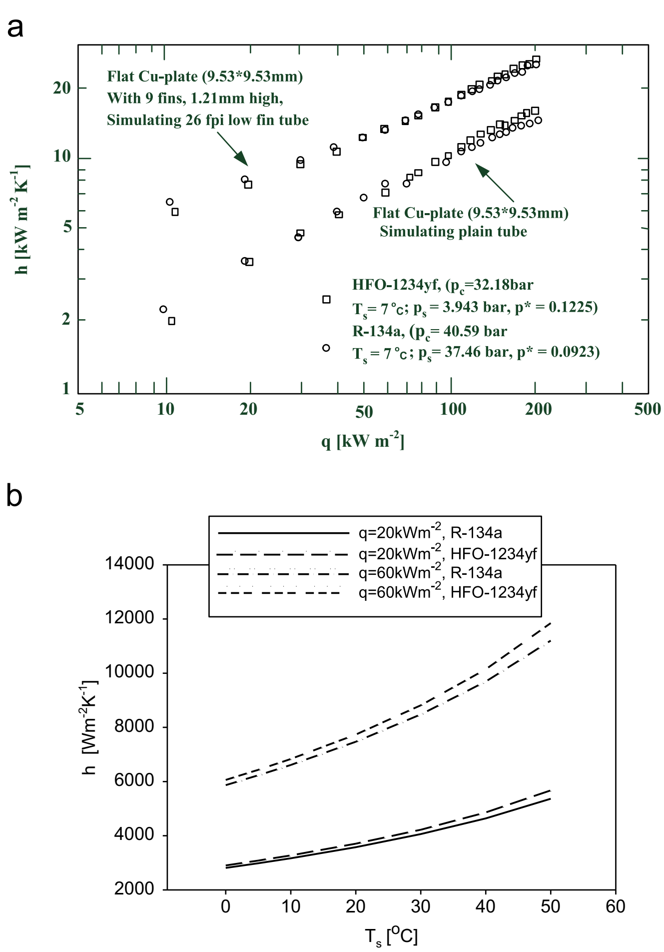


Fig. 3. Nucleate boiling HTCs of HFC-134a and HFO-1234yf on flat surfaces. (a) Nucleate boiling HTCs of HFC-134a and HFO-1234yf on two flat copper surfaces simulating a plain or low fin tube, respectively, [7]. (b) Comparison of the calculated nucleate boiling HTCs of HFC-134a and HFO-1234yf on flat plate using the Cooper correlation.

also made comparisons (smooth tube) with their condensation HTCs against the well accepted Nusselt's equation:

$$h_c = 0.728 \times \left[\frac{\rho_L(\rho_L - \rho_G) g i_{LG} k_L^3}{\mu_L (T_s - T_w) d_o} \right]^{1/4} \tag{1}$$

Table 2
Specification of the enhanced tube tested [8].

Tube type	Outside diameter (mm)	Fin height (mm)	Fin thickness (mm)		Fins/m
			At tip	At base	
Plain	19.05	–	–	–	–
Low fin	18.90	1.214	0.252	0.576	1024
Turbo-C	18.90	0.760	0.250	0.350	1654

Park et al. [8] had slightly modified the original Nusselt equation based on their previous study [19], as

$$h_{\text{predict}} = 0.79 \times \left[\frac{\rho_L(\rho_L - \rho_G) g i_{LG} k_L^3}{\mu_L (T_s - T_w) d_o} \right]^{1/4} \tag{2}$$

Their comparison (using Eq. (2)) revealed that the measured data for R-134a and HFO-1234yf were 9.0% and 27.1% larger than the predicted values. They argued that the relatively large deviation associated with HFO-1234yf were from the large uncertainties of various properties of HFO-1234yf. A similar calculation was made by the present author using Eq. (1) for plain tube with d_o = 19.05 mm and T_w = 20 °C. The calculated results in Fig. 4(b) show that the condensation HTCs for R-134a are much higher than that of HFO-1234yf (around 30–60%). It is not totally clear why the tested condensation HTC for R-134a and HFO-1234yf [8] are comparable for all the test tubes at the same condensation temperature. One of the possible reasons may be associated the large uncertainty of their measurements. This is because their test tube is quite short and the acquired heat transfer rate (temperature difference subtracted from the inlet and outlet of cooling water) and temperature difference between the surface and saturation temperature (T_s–T_w) are comparatively small. This is especially pronounced when enhanced tubes (low fin and turbo C) were used. In addition to the uncertainty, another possible explanation may be attributed to their relative short test length (L = 290 mm) which may cause some end effect (lateral conduction from the test tube to the flange) that inevitably promotes condensation. Note that most of properties influencing the condensation HTC suggest a lower condensation HTC of HFO-1234yf.

2.3. Results of in-tube evaporation

Saitoh et al. [9] conducted study for boiling heat transfer of the refrigerant HFO-1234yf flowing in a smooth small-diameter

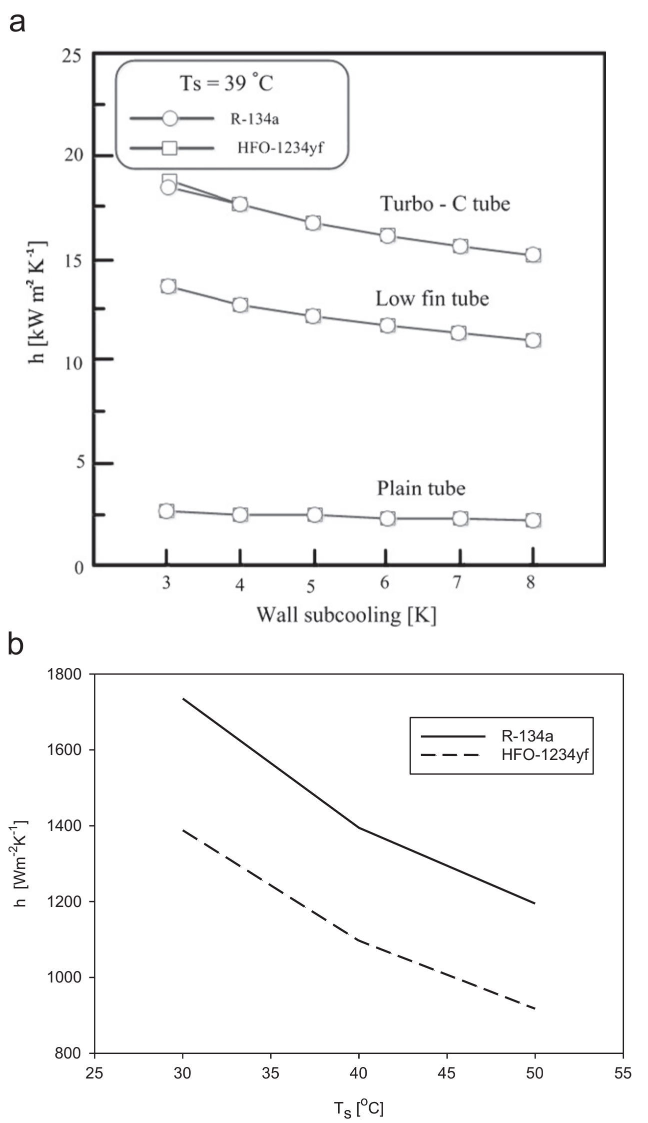


Fig. 4. Condensation HTC for R-134a and HFO-1234yf. (a) External condensation HTCs of R-134a and HFO-1234yf on various tubes [8]. (b) Comparison of the calculated condensation HTCs of R-134a and HFO-1234yf using Nusselt equation for plain tube.

horizontal tube (inner diameter (ID): 2 mm) and Li et al. [10] used similar test facility and identical test tube for comparing the HTC amid HFC-32 and HFO-1234yf. The test tube was heated by direct electrification using a DC power supply connected to two electrodes soldered at the flanges of the two ends of the test tube. Their experimental conditions are T_s=15 °C, q=6–24 kW m^{-2}, and G=100–400 kg m^{-2} s^{-1}. Fig. 5(a) shows the variation in the heat transfer coefficient against the vapor quality. The mass flux was kept at 200 kg m^{-2} s^{-1}; the measured results are for three different heat fluxes: 6, 12, and 24 kW m^{-2}, respectively. At the lowest heat flux of 6 kW m^{-2}, the measured heat transfer coefficient increased with the vapor quality, showing that the convective heat transfer intensifies with increasing quality. The dryout quality was about 0.8 and did not change with heat flux. Increasing the heat flux from 6 to 12 and 24 kW m^{-2} showed that the heat transfer coefficient increases with heat flux at low vapor quality; thus, nucleate boiling is the dominant heat transfer coefficient mechanism at low vapor quality. On the other hand, the detectable rise of HTC (heat transfer coefficient) vs. vapor quality for a low heat flux of 6 kW m^{-2} is associated with the change of flow pattern since annular flow may prevail at high quality region. However, as claimed by the authors who argues that nucleate boiling is dominant heat transfer process when q=12 and 24 kW m^{-2}, thereby showing a moderate change of HTC as vapor quality is increased. This seems feasible but the relative effect of heat flux, based on the test results of Saitoh et al. [9], is in fact much lower. A rough estimation of the heat flux dependency is about $h \sim q^{0.42}$ which is generally much lower than the pure nucleate boiling where $h \sim q^{06-0.7}$. In this sense, it is expected that convective evaporation still plays certain role rather than pure nucleate boiling.

Fig. 5(b) shows the effect of mass flux on the boiling heat transfer at a heat flux of 12 kW m^{-2}. The dryout occurs at a vapor quality of 0.8 for all the conditions. In the high quality region (>0.4), the heat transfer coefficients at both mass fluxes (200 and 400 kg m^{-2} s^{-1}) increased with the increasing vapor quality, and the heat transfer coefficient was higher at 400 kg m^{-2} s^{-1} than at 200 kg m^{-2} s^{-1}. At a mass flux of 100 kg m^{-2} s^{-1}, the effect of vapor quality on the heat transfer coefficient was weak. The results suggest that in the high vapor quality region, forced convective evaporation is dominant. In the lower quality region, $x<0.4$, the HTC is rather insensitive to change of mass flux, indicating a nucleate boiling dominant regime. Fig. 5(c) depicts a comparison between the boiling heat transfer performances of HFO-1234yf and R-134a at a mass flux of 300 kg m^{-2} s^{-1} and a heat flux of 12 kW m^{-2}. The figure shows that in the wide vapor quality region, the difference between the heat transfer coefficients of HFO-1234yf and R-134a is small, Saitoh et al. [9] attributed this to the small differences in their thermodynamic properties. In addition to this possible explanation, as explained earlier, the contribution of nucleate boiling for both refrigerants is about the same when q is small. Moreover, it will be shown in subsequent section that the flow patterns [12] for both fluids are virtually similar, thereby resulting in a comparable convective boiling performance. The present author also made a calculation of the convective boiling HTC between R-134a and HFO-1234yf at a saturation temperature of 10 °C with d_i=10 mm, q=20–40 kW m^{-2} using the well-known Chen correlation [20]. The calculated results indicated that the difference between R-134a and HFO-1234yf is very small. Mortada et al. [11] performed an experiment for HFO-1234yf and R-134a in a 1.1 mm rectangular channel with rather small mass flux of 20–100 kg m^{-2} s^{-1} and heat flux from 2–15 kW m^{-2}. However, their results showed that the HTC for HFO-1234yf is lower than that of R-134a as much as 40% and convective boiling is the major heat transfer mechanism even at this mini-size tube. Notice that nucleate boiling is the major heat transfer mechanism in most published works in mini-size or micro-size tubes. The results are contradictory to previous results. It is not totally clear why the test results of Mortada et al. [11] showed a different trend.

Saitoh et al. [9] also measured two-phase pressure drop (ΔP). The pressure drops were compared with the Lockhart Martinelli correlation, which defines the pressure drop as:

$$-\left(\frac{dP}{dz}\right) = -\left(\frac{dP}{dz}\right)_L \phi_L^2 = -\left(\frac{dP}{dz}\right)_G \phi_G^2 \quad (3)$$

where ϕ_L and ϕ_G are the two-phase multipliers in the liquid and gas phases, respectively. The multipliers are defined as $\phi_L=(1+C/X+1/X^2)^{0.5}$ and $\phi_G=(1+CX+X^2)^{0.5}$, where X is the Lockhart Martinelli parameter, which is the square root of the ratio between the pressure drop assuming liquid flow alone and assuming gas flow alone. When the liquid and gas phases are turbulent, C=20; when the liquid phase is laminar and the gas phase is turbulent, C=12. Fig. 5(d) shows the measured pressure drops and those predictions using the Lockhart Martinelli correlation. The measured pressure drops agreed well with the Lockhart Martinelli correlation.

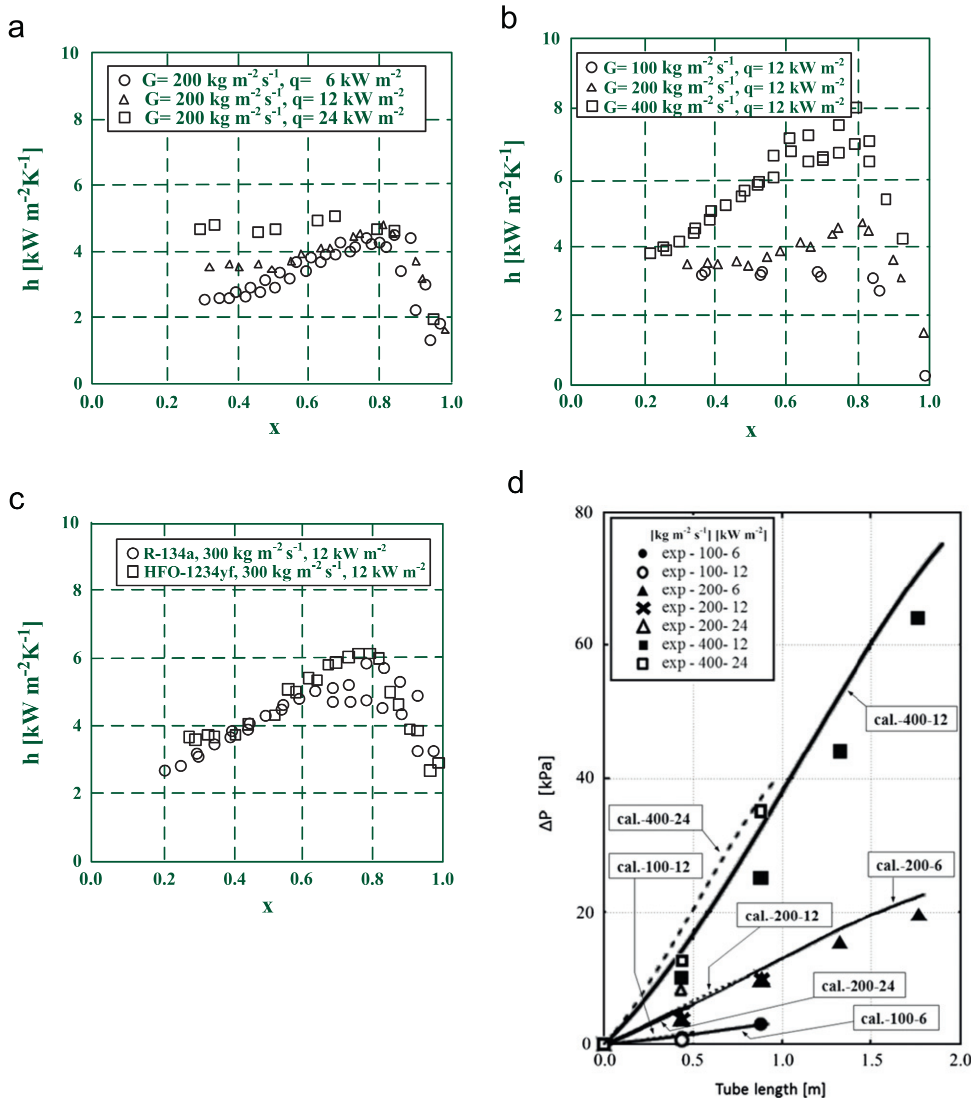


Fig. 5. In-tube convective boiling heat transfer coefficients and pressure drop data of Saitoh et al. [9]. (a) Effect of heat flux on local heat transfer coefficient for HFO-1234yf. (b) Effect of mass flux on local heat transfer coefficient for HFO-1234yf. (c) Comparison of heat transfer coefficients between HFO-1234yf and R-134a at mass flux of 300 kg m^{-2} s and at a heat flux of 12 kW m^{-2}. (d) Comparison of pressure drops between measured values and values calculated by the Lockhart Martinelli correlation for HFO-1234yf.

Despite the Lockhart Martinnlli correlation seems to give very excellent prediction of the pressure drop upon Saitoh et al.'s measurement. It should be mentioned that the results are applicable only for a 2-mm tube. Padilla et al. [12] performed flow visualization as well as pressure drop measurement for three working fluids—R-410A, R-134a, and HFO-1234yf. The tube diameter (D) varies from 7.90 to 10.85 mm. The mass velocity ranges from 187 to 1702 kg m^{-2} s^{-1} and the saturation temperatures from 4.8 to 20.7 °C. For a saturation temperature of 10 °C and D=6.7 mm, the corresponding flow pattern for G=300 kg m^{-2} s^{-1} and G=500 kg m^{-2} s^{-1} subject to vapor quality for R-134a and HFO-1234yf are depicted in Figs. 6 and 7. The different flow regimes observed are: slug, intermittent and annular flows. The observed flow patterns, for the same vapor quality, saturation temperature, mass flux, and tube diameter, are virtually the same amid R-134a and HFO-1234yf. This is desirable since HFO-1234yf was designed so that not only its properties would be close to those of R-134a but also equipped with the same flow phenomena. Analogous flow patterns amid R-134a and HFO-1234yf in a horizontal return bend was also reported by Padilla et al. [13].

Their measured results of pressure drop are also compared against 10 well-known two-phase frictional pressure drop prediction methods. However, unlike that of Saitoh et al. [9] who reported the Lockhart Martinnlli correlation shows excellent predictive ability, Padilla et al. [13] shows that the predictive ability of the Lockhart Martinnlli correlation is actually among the poorest one. Padilla et al. [12] showed that the Müller-Steinhagen and Heck correlation [21] gives the best predictive capability. The mean absolute error is near 19% and the mean relative error is around ±3%. Typical comparison is shown in Fig. 8. Although the method proposed by Müller-Steinhagen and Heck [21] is a method which has been developed without considering flow pattern effects on the process, this method gives the best prediction for intermittent and annular flows, but also for their entire database.

2.4. In-tube condensation

Col et al. [14] conducted experiments for measurement of local heat transfer coefficients during condensation of HFO-1234yf within a single circular 0.96 mm diameter microchannel at

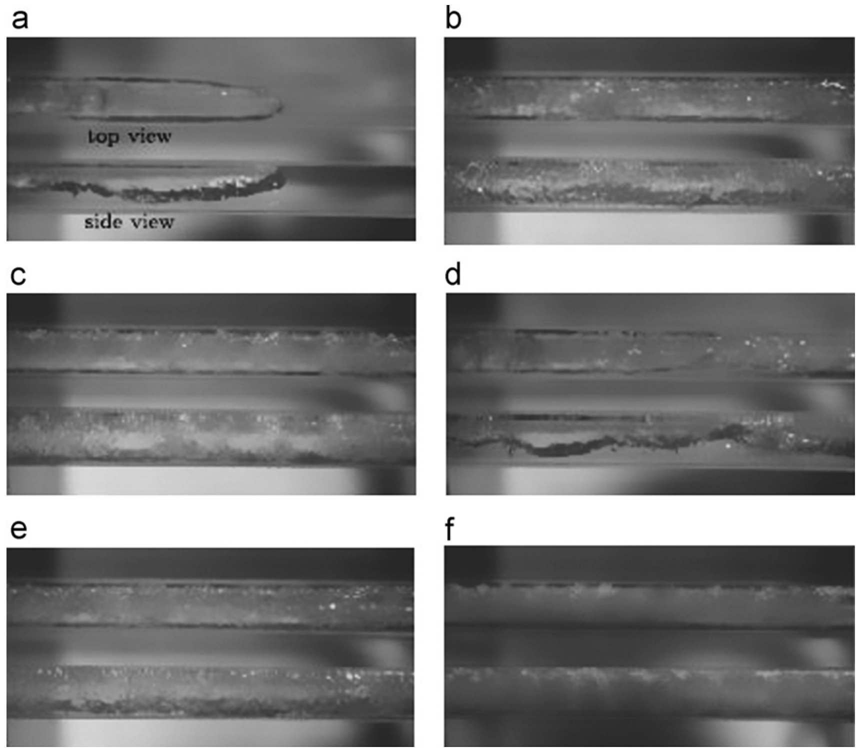


Fig. 6. Top and side views of the R-134a flow patterns for T_s=10 °C and D=6.70 mm [12]. (a) Slug flow, x=0.05, G=300 kg m^{-2} s^{-1}. (b) Intermittent flow, x=0.05, G=300 kg m^{-2} s^{-1}. (c) Annular flow, x=0.6, G=300 kg m^{-2} s^{-1}. (d) Intermittent flow, x=0.05, G=500 kg m^{-2} s^{-1}. (e) Intermittent flow, x=0.2, G=500 kg m^{-2} s^{-1}. (f) Annular flow, x=0.6, G=500 kg m^{-2} s^{-1}.

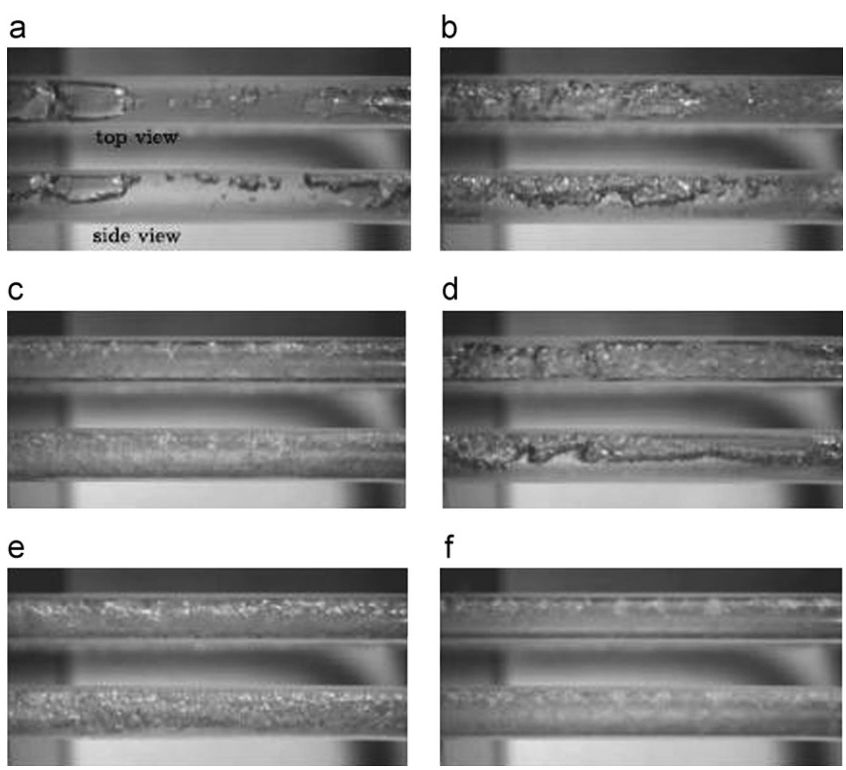


Fig. 7. Top and side views of the HFO-1234yf flow patterns for T_s=10 °C and D=6.70 mm [12]. (a) Slug flow, x=0.05, G=300 kg m^{-2} s^{-1}. (b) Intermittent flow, x=0.05, G=300 kg m^{-2} s^{-1}. (c) Annular flow, x=0.6, G=300 kg m^{-2} s^{-1}. (d) Intermittent flow, x=0.05, G=500 kg m^{-2} s^{-1}. (e) Intermittent flow, x=0.2, G=500 kg m^{-2} s^{-1}. (f) Annular flow, x=0.6, G=500 kg m^{-2} s^{-1}.

40 °C saturation temperature and compares them to the ones of R-134a. Condensation tests are carried out at mass fluxes ranging between 200 and 1000 kg m^{-2} s^{-1}. They reported sufficient heat transfer deteriorations for the HFO-1234yf as compared to the ones of R-134a. In Fig. 9 the local heat transfer coefficients and at three different mass velocities are compared to the ones of

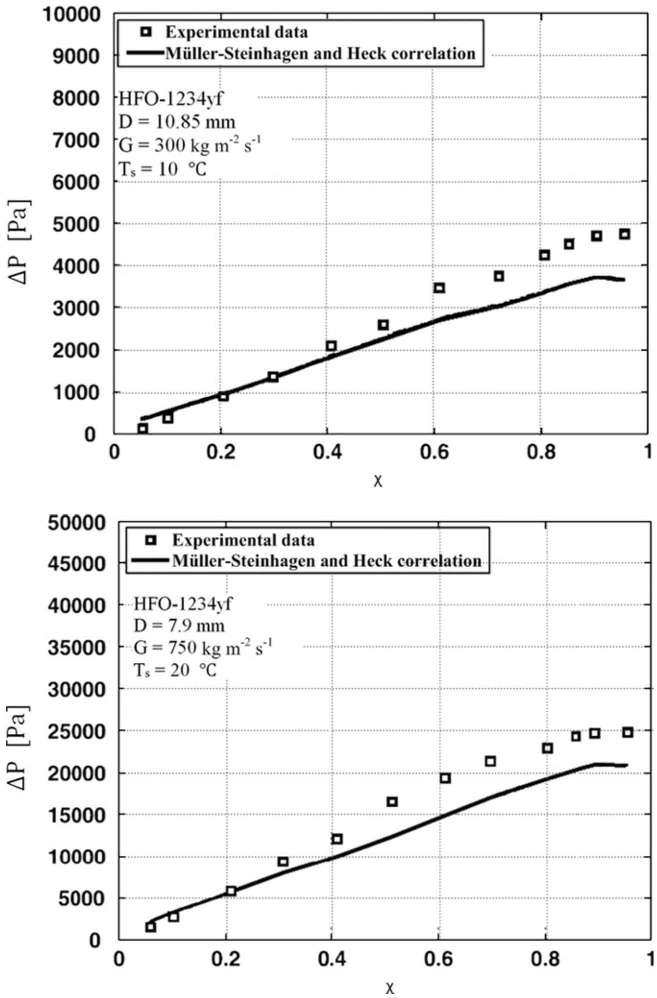


Fig. 8. Experimental pressure drop in straight tubes as a function of the vapor quality compared to different prediction methods [12].

R-134a at the same operating conditions. Except for the lowest values of vapor quality, R-134a displays a heat transfer coefficient higher than HFO-1234yf for all three values of mass velocities. At a mass flux of 200 kg m^{-2} s^{-1} (Fig. 9(a)), the heat transfer coefficient of HFO-1234yf is lower than that of R-134a by 15% at 0.4 vapor quality and by 30% at 0.8 vapor quality. One of the explanations about the pronounced difference in HTC between HFO-1234yf and R-134a at a higher vapor quality region is due to film thickness on the periphery. Notice that at higher vapor quality regime the annular flow prevails. On the other hand, the liquid density for R-134a is about 11% higher than that of HFO-1234yf (see Table 1b). This implies a thinner film thickness of R-134a provided the vapor quality is the same, thereby leading to a higher HTC for R-134a.

A similar trend is found at 400 and 800 kg m^{-2} s^{-1} mass velocity as shown in Fig. 9(b) and (c). When comparing the heat transfer coefficient of HFO-1234yf to the one measured for R-134a, one can see that the latter fluid displays a higher coefficient at the same operating conditions, and this is related to the different properties of the two fluids. Additionally, as aforementioned in the nucleate boiling section, the higher reduced pressure of HFO-1234yf also contributed to decrease the associated condensation heat transfer coefficient, this can be easily seen from the well-known Shah correlation [22] where:

$$h_c = h_L\left(1+\frac{3.8}{Z}\right) \tag{4}$$

where

$$Z = \left(\frac{1-x}{x}\right)^{0.8}(P^*)^{0.4} \tag{5}$$

$$h_L = \frac{k_L}{d_i}0.023\left(\frac{G(1-x)d_i}{\mu_L}\right)^{0.8}\mathrm{Pr}^{0.4} \tag{6}$$

A similar calculation for comparing the in-tube condensation HTC for R-134a and HFO-1234yf using the Shah correlation is also made. And it clearly substantiated the measured results of Col et al. [14] who shows the HTC of HFO-1234yf is inferior to that of R-134a. Test results by Wang et al. [15] also unveiled similar trend.

Fig. 9(d) shows the total experimental pressure drop measured with HFO-1234yf and R-134a at 40 °C saturation temperature with three different values of mass velocity: 400, 600 and 800 kg m^{-2} s^{-1}. It can be seen that the fluid HFO-1234yf displays a lower pressure drop by 10–12% as compared to that of R-134a, at the same operating conditions. This may be easily understood since the reduced pressure of HFO-1234yf is 20% greater than that of R-134a at 40 °C saturation temperature (see Table 1a and 1b). A similar result was also reported by Park et al. [23] who condensed R-1234ze(E) within a multi-port MAC condenser with an internal hydraulic diameter of 1.45 mm. They reported that the heat transfer performance of HFO-1234ze(E) was about 15–25% lower than for R-134a. However, experimental flow boiling heat transfer results with R1234ze(E) by Tibiricá et al. [24] for horizontally test tubes having 1.0 and 2.2 mm I.D. (internal diameter) stainless steel tubes shows a comparable performance amid HFO-1234ze(E) and R-134a. The reason is analogous to the aforementioned discussion in nucleate boiling. Pressure drop measurements for R-134a and HFO-1234yf by Padilla et al. [13] also depicted analogous results.

3. Conclusions

This short overview gives the heat transfer performance for refrigerant HFO-1234yf which is made to substitute R-134a. At present, the associated studies concerning the heat transfer performance is still limited. However, based on the limited information, the associated comparison of heat transfer performance, including nucleate boiling, in-tube convective evaporation, external condensation, in-tube condensation, and flow pattern, between HFO-1234yf and R-134a is summarized as:

(a) For nucleate boiling with $q < 200$ kW m^{-2}, the heat transfer coefficients (HTC) for smooth surface between R-134a and HFO-1234yf are comparable. And the HTC of HFO-1234yf is lower than that of R-134a when q is greater than 200 kW m^{-2}. The critical heat flux of HFO-1234yf is about 20–40% lower than that of R-134a.
(b) For microporous surface, the nucleate HTC for R-134a is moderately higher than those of HFO-1234yf.
(c) For external condensation, the only database shows that the HTC between HFO-1234yf and R-134a is negligible. However, it is found that the major thermophysical properties influencing condensing HTC suggest a lower HTC of HFO-1234yf. It is therefore recommended that further verifications should be made.
(d) For in-tube convective boiling, the experimental data showed that the difference in HTC for HFO-1234 and R-134a is quite small, and for the same flow condition (vapor quality, mass velocity, saturation temperature, tube diameter), the corresponding flow pattern for R-134a and HFO-1234yf are

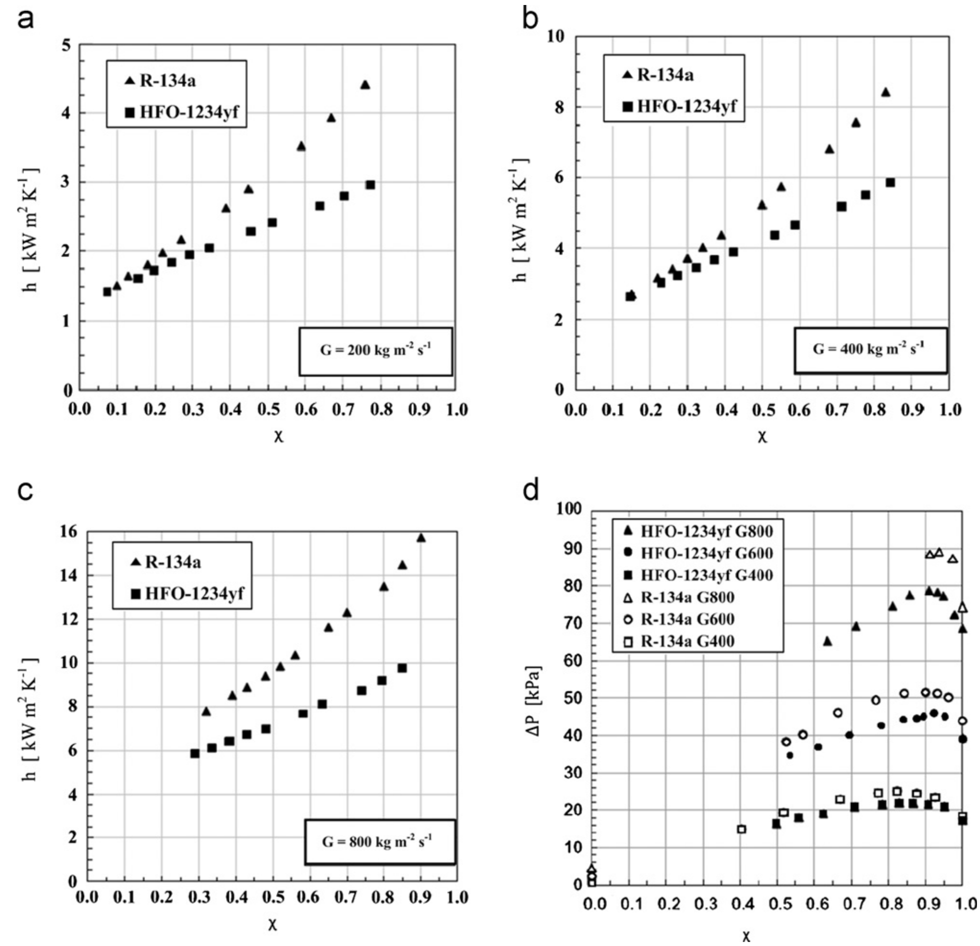


Fig. 9. Experimental local heat transfer coefficient and pressure drops versus vapor quality for HFO-1234yf and R-134a at 200, 400 and 800 kg m^{-2} s^{-1} mass velocity (from Col et al. [14]). (a) h vs. x for G=200 kg m^{-2} s^{-1}. (b) h vs. x for G=400 kg m^{-2} s^{-1}. (c) h vs. x for G=800 kg m^{-2} s^{-1}. (d) ΔP vs. x for G=400, 600 and 800 kg m^{-2} s^{-1}.

virtually the same. However, some test results in mini-channel indicated that the HTC for HFO-1234yf is much higher than that of R-134a. This result also requires further validation.

(e) For in-tube condensation, it is found that the condensation HTCs for HFO-1234yf are inferior to those of R-134a, and the difference increases with the rise of vapor quality.

(f) The predictive correlations applicable for pressured drop for HFO-1234yf are not consistent, it is probably attributed to the difference in tube diameter in the publications.

Acknowledgement

The author would like to express gratitude for supporting funding from the National Science Council of Taiwan (100–2221-E-009–087-MY3).

References

[1] Papasavva S, Luceken DJ, Waterland RL, Taddonio KN, Andersen SO. Estimated 2017 refrigerant emissions of 2,3,3,3-tetrafluoropropene (HFC-1234yf) in the United States resulting from automobile air conditioning. Environmental Science and Technology 2009;43:9252–9.

[2] Akasaka R, Tanaka K, Higashi Y. Thermodynamic property modeling for 2,3,3,3-tetrafluoropene (HFO-1234yf). International Journal of Refrigeration 2010;33:52–60.

[3] Lee Y, Jung D. A brief performance comparison of R1234yf and R134a in a bench tester for automobile applications. Applied Thermal Engineering 2012;35:240–2.

[4] Zilio C, Brown JS, Schiochet G, Cavallini A The refrigerant R1234yf in air conditioning systems, Energy; 36:6110–6120.

[5] Jarall S. Study of refrigeration system with HFO-1234yf as a working fluid. International Journal of Refrigeration 2012;35:1668–77.

[6] Moreno G, Narumanchi S, King C. Pool boiling heat transfer characteristics of HFO-1234yf with and without microporous-enhanced surfaces. Proceedings of the ASME 2011 international mechanical engineering congress & exposition IMECE2011 November 11–17, 2011, Denver, Colorado, USA, paper no. IMECE2011-64002.

[7] Park KJ, Jung D. Nucleate boiling heat transfer coefficients of R1234yf on plain and low fin surfaces. International Journal of Refrigeration 2010;33:553–7.

[8] Park KJ, Kang DG, Jung D. Condensation heat transfer coefficients of R1234yf on plain, low fin, and Turbo-C tubes. International Journal of Refrigeration 2011;34:317–21.

[9] Saitoh S, Dang C, Nakamura Y, Hihara E. Boiling heat transfer of HFO-1234yf flowing in a smooth small-diameter horizontal tube. International Journal of Refrigeration 2011;34:1846–53.

[10] Li M, Dang C, Hihara E. Flow boiling heat transfer of HFO1234yf and R32 refrigerant mixtures in a smooth horizontal tube: Part I. Experimental investigation. International Journal of Heat and Mass Transfer 2012;55:3437–46.

[11] Mortada S, Zoughaib A, Arzano-Daurelle C, Clodic D. Boiling heat transfer and pressure drop of R-134a and R-1234yf in minichannels for low mass fluxes. International Journal of Refrigeration 2011;34:317–21 2012 35:962-973.

[12] Padilla M, Revellin R, Haberschill P, Bensafi A, Bonjour J. Flow regimes and two-phase pressure gradient in horizontal straight tubes: experimental results for HFO-1234yf R-134a and R-410A. Experimental Thermal and Fluid Science 2011;35:1113–26.

[13] Padilla M, Revellin R, Bonjour J. Two-phase flow visualization and pressure drop measurements of HFO-1234yf and R-134a refrigerants in horizontal return bends. Experimental Thermal and Fluid Science 2012;39:98–111.

[14] Col DD, Torresin D, Cavallini A. Heat transfer and pressure drop during condensation of the low GWP refrigerant R1234yf. International Journal of Refrigeration 2010;33:1307–18.

[15] Wang L, Dang C, Hihara E. Experimental study on condensation heat transfer and pressure drop of low GWP refrigerant HFO1234yf in a horizontal tube. International Journal of Refrigeration 2012;35:1418–29.
[16] Thome J, Wolverine engineering data book III, chapter 9.
[17] Tanaka K, Higashi Y. Thermodynamic properties of HFO-1234yf (2,3,3,3-tetrafluoropropene). International Journal of Refrigeration 2010;33:474–9.
[18] Cooper MG. Heat flow rates in saturated nucleate pool boiling—a wide-ranging examination using reduced properties. Advances in heat transfer, 16. Academic Press; 1984 pp. 157-239.
[19] Jung D, Chae S, Bae D, Oho S. Condensation heat transfer coefficients of flammable refrigerants. International Journal of Refrigeration; 27:314–317.
[20] Chen JC. Correlation for boiling heat transfer to saturated fluids in convective flow. Industrial & Engineering Chemistry Process Design 1966;5:322.
[21] Müller-Steinhagen H, Heck K. A simple friction pressure drop correlation for two-phase flow pipes. Chemical Engineering and Processing 1986;20: 297–308.
[22] Shah MM. A general correlation for heat transfer during film condensation inside pipes. International Journal Heat Mass Transfer 1979;22:547–56.
[23] Park JE, Vakili-Farahani F, Consolini L, Thome JR. Experimental study on condensation heat transfer in vertical minichannels for new refrigerant R1234ze(E) versus R134a and R236fa. Experimental Thermal and Fluid Science 2011;35:442–54.
[24] Tibiricá CB, Ribatski G, Thome JR. Flow boiling characteristics for R1234ze(E) in 1.0 and 2.2 mm circular channels. Journal of Heat Transfer 2012;134:020906-1–8.